Numerical analysis of hexagonal solid-core photonic crystal fibers

Peter Blattnig, Valerio Romano, Willy Lüthy, Thomas Feurer

January 31, 2006

Abstract

The basic properties of hexagonal solid-core fibers are reviewed. The influence of geometry (hole diameter d, pitch Λ and number of rings N_r) on losses and dispersion is investigated. Also, a definition of single modedness is explained. Finally, a possible configuration of a preform is presented. The aim is the creation of a large area endlessly single mode fiber whose properties can be compared with a commercial product.

1 Introduction

There are essentially two different kinds of photonic crystal fibers: Solid core- and hollow-core microstructered fibers (MOFs). Solid core MOFs work on the principle of modified total internal reflection while the guiding mechanism in hollow MOFs is based on band gaps. We will concentrate on hexagonal solid core MOFs. The main parameter of a fiber is its effective index of refraction n_{eff} whose real part contains the dispersion information D, whereas the imaginary part allows the calculation of the losses L.

$$L = \frac{40\pi}{ln(10)\lambda} Im(n_{eff}) \tag{1}$$

$$D = -\frac{\lambda}{c}\frac{\partial^2 Re(n_{eff})}{\partial\lambda^2} \tag{2}$$

The effective index is composed of the material part and the geometric part: $n_{eff} = n_{eff}^{mat} + n_{eff}^{geom}$. For a given material, only the geometric part can be influenced. An additional source of losses results from the bending of the fiber. These losses are difficult to model but order of magnitude results can be obtained via the effective area of the modes [9].

2 Used software

To calculate the effective indices, the free software CUDOS [4] was used. This program is an implementation of the multipole method which is very efficient for calculations on fibers with circular inclusions. Higher order modes were calculated with the commercial software BEAMPROP [1] which is an implementation of the beam propagation algorithm. To test the consistency of the two methods, they were both applied to the same fiber geometry and the results were compared. Additional verification resulted from comparison with [11] which used a fully vectorial finite element-solver.

3 General properties of hexagonal solid-core fibres

The geometry of a hexagonal fiber (of uniform hole-size) is completely described by the diameter of the air holes d, the distance between the centers of two adjacent holes Λ (pitch) and the number of rings N_r. Fig.1 shows a configuration with three rings.

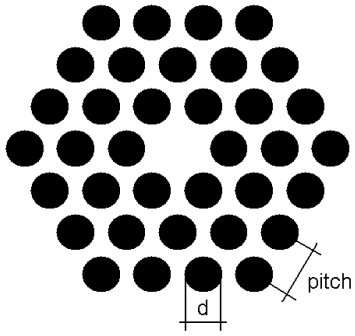

Figure 1: Hexagonal array with N_r=3, definition of fiber parameters d and Λ (pitch)

The influence of the number of rings on the effective index was calculated for some exemplary choices of N_r and d/Λ. The wavelength was held constant at 1064nm so that the material index remains constant. The influence on the losses ($im(n_{eff})$) is shown in Fig.2.

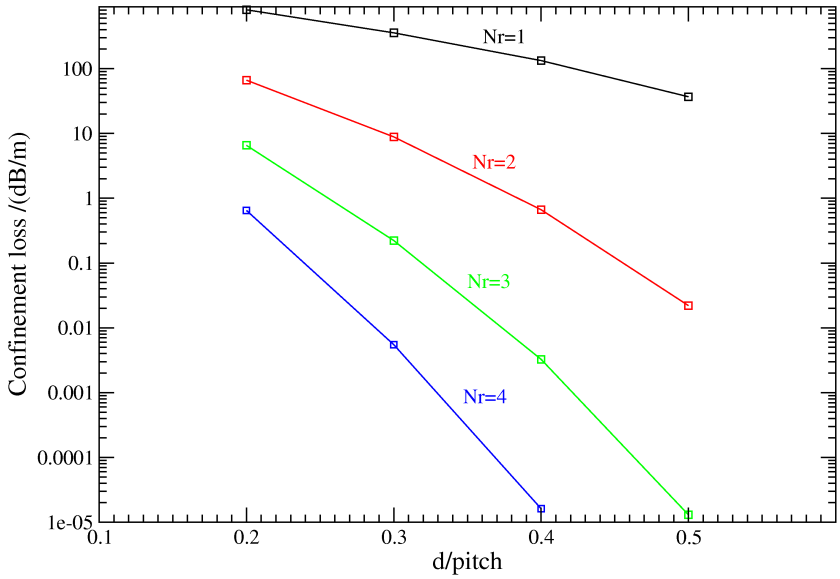

Figure 2: Losses as a function of $d/pitch$ and N_r, $\Lambda = 8\mu m$, λ=1064nm

A simple but useful model of a solid core MOF is to assume the cladding to be homogeneous with index $n_{FSM} = \beta_{FSM}/k_0$, where β_{FSM} is the propagation constant of the fundamental space

filling mode. This is the mode with the highest β of an infinite crystal with the same d and Λ as in the fiber, but without missing hole. Then the losses become smaller as the filling ratio d/Λ becomes larger until, in the extreme, the core is surrounded by a cladding of air. This model is exact only in the limit of $N_r \to \infty$ where the modes can become completely confined (as in a step index fiber) and so the losses also decrease as a function of N_r. It can be shown [13] (and roughly seen in Fig.2 by the approximately equal distances at constant d/Λ) that the losses decrease exponentially with the number of rings.
For d/Λ =constant, the losses decrease with increasing Λ (Fig.3). Increasing Λ is equivalent to scaling the overall fiber dimension and we expect a decrease of the losses because field boundary interactions become less relevant for large fibers.

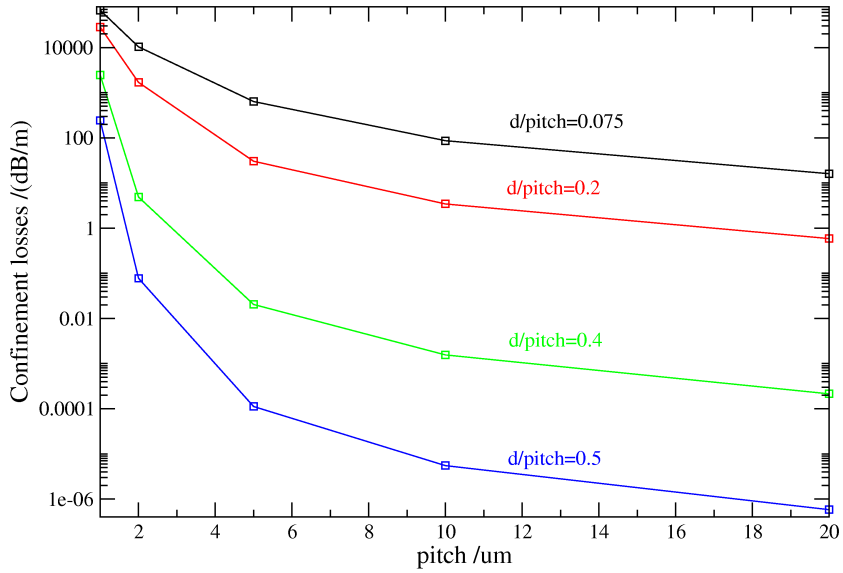

Figure 3: Losses for constant d/Λ and N_r =3, λ=1064nm

However, the situation looks different if bending losses have to be taken into account. The larger the fiber, the larger the gaps between the holes where light can leak out of the fiber.
The dependence of the real part of n_{eff} on N_r is shown in Fig.4.

The convergence is very fast. For smaller values of Λ the convergence is slower ([15]) but for all practical purposes $N_r \geq 4$ is sufficient.

4 Definition of single modedness

Because all modes in a solid core MOF are leaky, there is no unique definition of single modedness. A possible approach is to compare the losses of the fundamental mode with those of the other modes and to require the energy of the fundamental mode to be dominant after propagation of a predefined length. This procedure is applied in [12]. While this definition is very useful from a practical point of view, it is dependent on the length of the fiber.

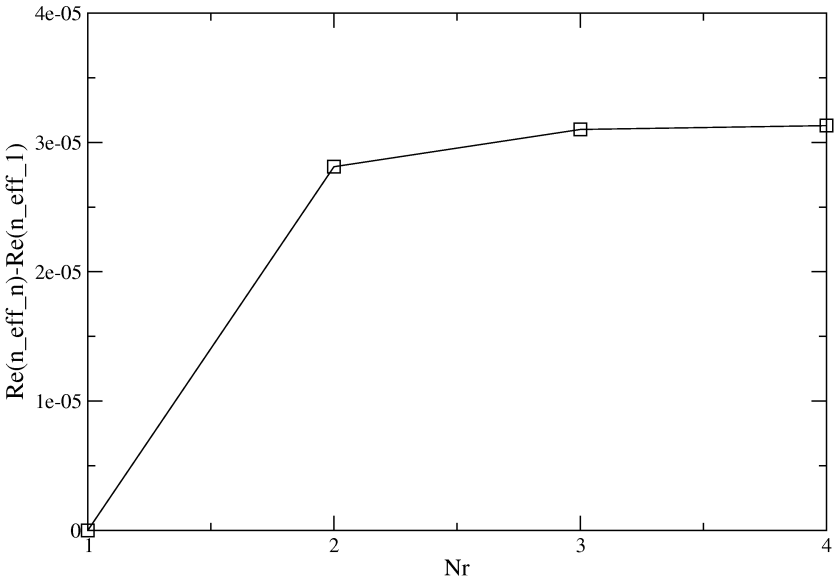

Figure 4: $Re(n_{eff}(N_r = n) - n_{eff}(N_r = 1))$ as a function of N_r, $\Lambda = 8\mu m$, λ=1064nm

Another definition that is independent of fiber-length is based on the losses of the second mode. Fig.5 shows $Im(n_{eff})$ of the second mode as a function of wavelength.

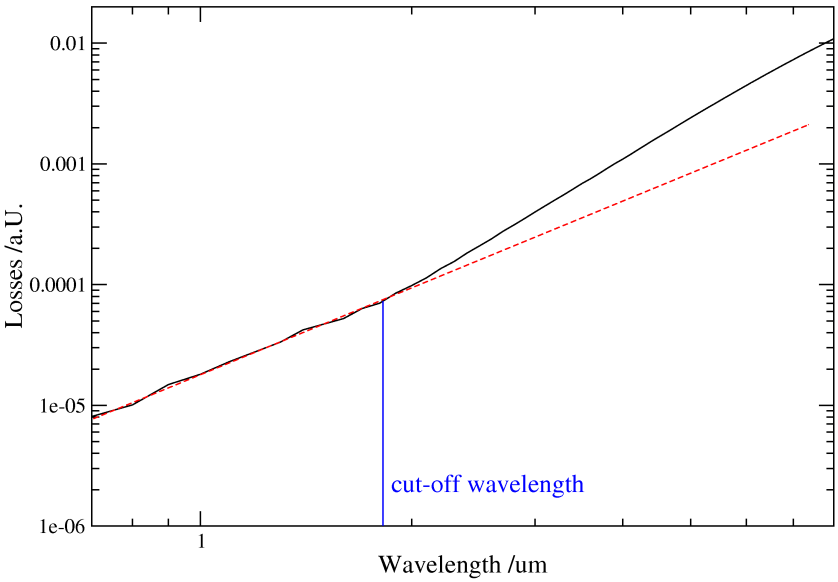

Figure 5: $Im(n_{eff})$ of the second mode

The wavelength where the slope of the curve changes marks a transition into a wavelength region

where the losses rise rapidly with increasing wavelength. The second derivative of $Im(n_{eff})$ shows a maximum at the so called cut-off wavelength λ_c. At the cut-off wavelength, the second mode changes from a well confined mode to a cladding filling mode with correspondingly higher losses.
The locus of all pairs (d/Λ,λ_c/Λ) defines a transition line in a phase diagram Fig.6. A fit to this transition as calculated by [15] is $2.8(\frac{d}{\Lambda} - 0.406)^{0.89}$.

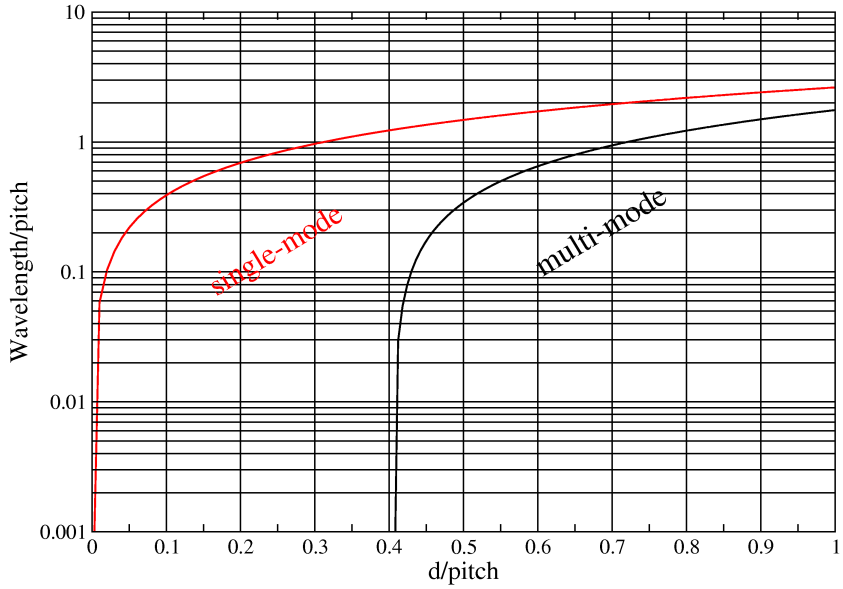

Figure 6: Cut-off phase-diagram

Values of d/Λ below 0.406 lead to single mode. However, if the fiber is very short, this definition declares fibers as single mode that do not discriminate much between the fundamental and the higher modes.
The second transition line in Fig.6 represents the cut-off of the fundamental mode which is no exception to the rule that all modes are leaky ($2.63(\frac{d}{\Lambda})^{0.83}$ as calculated by [15].)
While the definition of the cut-off wavelength relies on a change in the losses of a fiber, this change is not the cause but just a consequence of the change of the mode profiles effective area. Its therefore possible to calculate the cut-off wavelength by numerical methods that cannot account for losses, as for example the plane wave decomposition method used in the calculations of bandstructures of photonic crystals. For a classical step index fiber, the criterion for singlemodedness is given by

$$V = \frac{2\pi\rho}{\lambda}\sqrt{n_{co}^2 - n_{cl}^2} \leq 2.405 \tag{3}$$

where n_{co}, n_{cl} and ρ are the core index, the cladding index and the core radius respectively. V is called the normed frequency. V is inversely proportional to the wavelength and as such has no upper bound. If n_{cl} is replaced by n_{FSM} and ρ by $\Lambda/\sqrt{3}$, it is shown ([7]) that this relation still holds. In contrast to the step index fiber, the cladding index is not constant and the value of V can have an upper bound.

Fig.7 was calculated using an analytic expression of n_{FSM} fitted to calculations of [10].

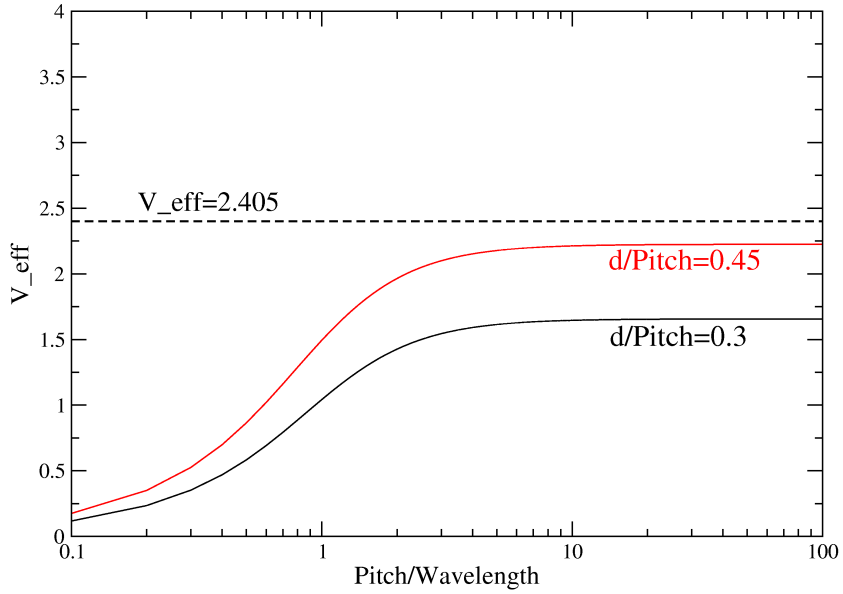

Figure 7: Normed frequency V for two different fibers

Fig.8 shows a mode profile of the second mode before and after crossing the cut-off boundary along a line of constant d/Λ =0.466. These calculations were performed by the plane-wave method implementation BANDSOLVE [1].

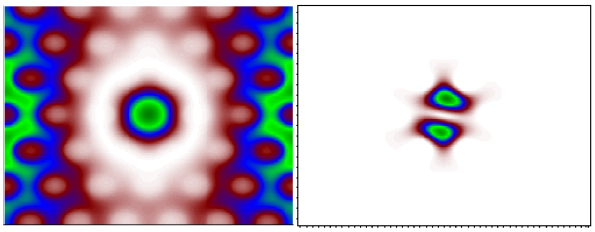

Figure 8: Second order mode: Cladding mode and confined mode

For large area applications it might be tempting to enlarge the core area by omitting not just one hole, but the first ring as well. While this leads indeed to a larger effective area, it also reduces the range of parameters for single mode operation [6] as shown in Fig.9 ($4.432(\frac{d}{\Lambda}-0.035)^{1.045}$). The hole sizes would have to be rather small, so that the bending-losses could become a real issue for fibers of only a few rings.

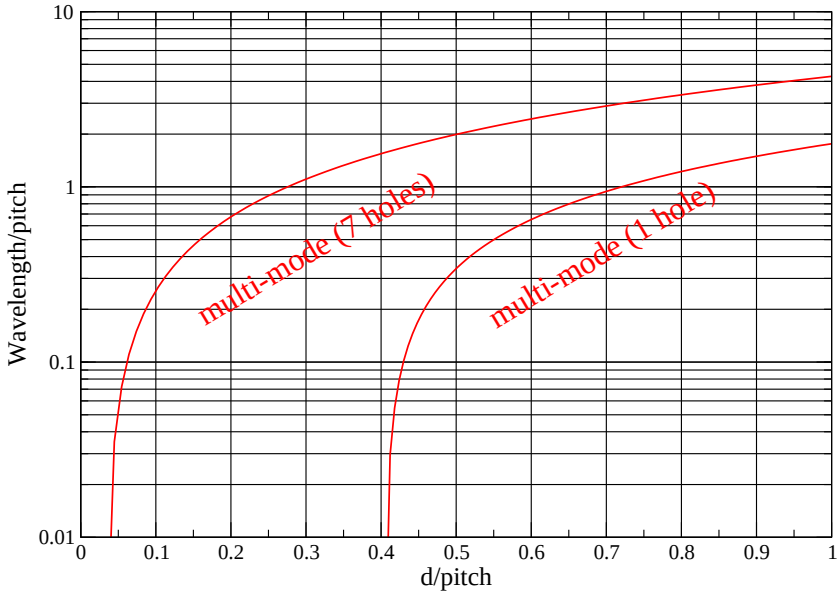

Figure 9: Phase diagram for 1 and 7 central holes missing

5 Dispersion properties

As in the case of the losses, it is possible to change the dispersion properties of a MOF by changing the geometric parameters. In what follows, we consider only the geometric contribution to the dispersion (n_{eff}^{mat} =constant). Because n_{eff} is dimensionless, the dispersion relation can only depend on d, Λ and λ through dimensionless ratios [5]: D(d,Λ,λ)=D(d/λ,Λ/λ). This leads to a relation between the dispersion curves of scaled fibers [15] which can save a lot of computation time.

$$D(\lambda, \Lambda/\Lambda_{ref}, f) = \frac{\Lambda_{ref}}{\Lambda} D(\lambda\Lambda_{ref}/\Lambda, 1, f) \tag{4}$$

Where f is the constant filling ratio d/Λ and Λ_{ref} is the pitch of the fiber for which the calculations were originally made. Fig.10 shows the dispersion curve of a MOF with $\Lambda = 8\mu m$, $d/\Lambda = 0.466$ and that of a scaled version with half that dimensions. There is no such scaling property relating fibers of different d/Λ [15].

If the material part of the dispersion is taken into account, the total dispersion of the above fiber will be dominated by this [12]. This is to be expected for large area fibers because a large part of the field propagates in bulk silica. The really interesting domain in the phase diagram where dispersion compensation is possible is near the domain boundary of the single mode regime [15].

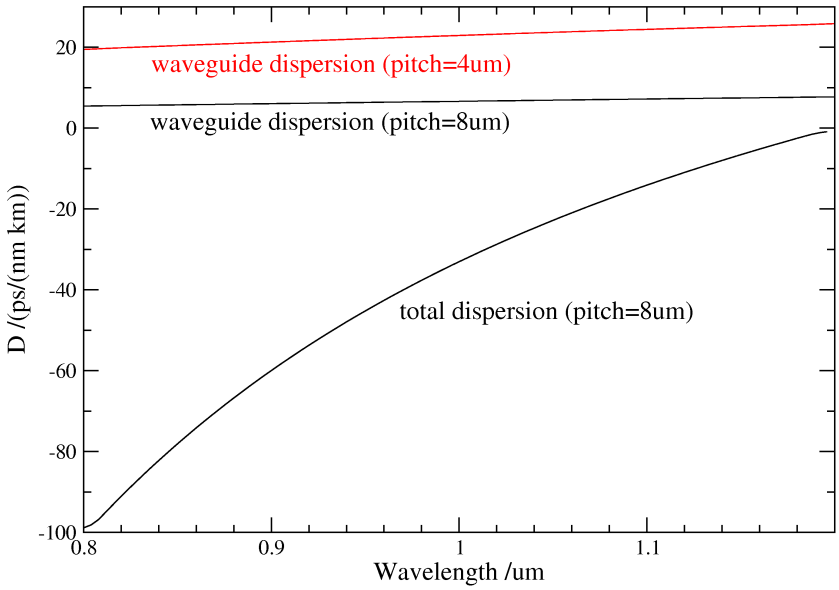

Figure 10: Dispersion relation for $\Lambda = 8\mu m, 4\mu m$ and d/Λ =0.466

6 Recommendations of a preform

A set of fiber parameters was chosen that coincides with that of the commercially available fiber ESM-12-01 of [3] in order to compare the measured fiber properties. The parameters are $\Lambda = 8\mu m$ and $d/\Lambda = 0.46$. The data-sheet suggests, that the losses of this fiber are dominated by the intrinsic losses (absorption, Rayleigh scattering). This is also consistent with the calculations in Fig.2. Although the parameters are located in the multimode regime Fig.6, [12] shows that the higher modes have essentially died out after a length of just one meter. A possible preform configuration is shown in Fig.11.

The dimensions of the tubes is D=3mm and d=1.4mm leading to $d/\Lambda = 0.4666....$ This filling ratio can be made smaller during the drawing process. A second approach is the stacking of slabs with milled grooves along the fiber axis Fig.12. This allows the selection of a wide range of hole geometries. The influence of this degree of freedom has yet to be investigated.

The effective area of this fiber at 1064nm was calculated to be $A_{eff} = 273\mu m^2$. It has to be added, that the above calculations were all performed with infinite cladding. The presence of a coating can modify the loss characteristics considerably.

7 Summary

A review of the key properties of hexagonal single mode fibers has been given. The necessary calculations were performed with the multipole-method and the beam-propagation-method. Based on these studies, a preform for the fabrication of a large area fiber is suggested.

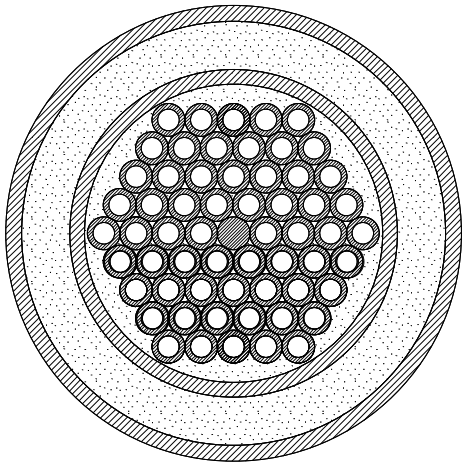

Figure 11: Preform after the stack-and-pull method, gaps filled with sand

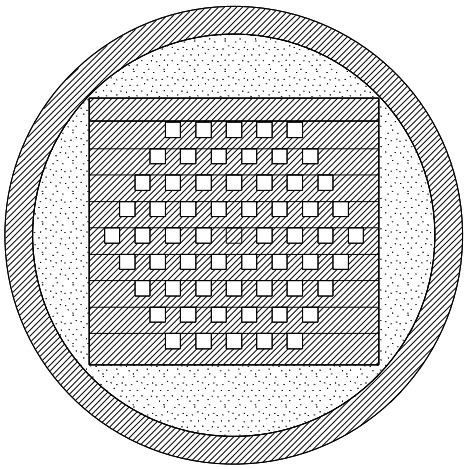

Figure 12: Preform made of stacked slabs, gaps filled with sand

References

[1] BEAMPROP , R-soft design group, www.rsoftdesign.com

[2] Birks T.A., Knight J.C., Russell P.St.J. (1997), Endlessly single-mode photonic crystal fiber, Optics Letters, Vol. 22, No. 13, July 1, pp. 961-963

[3] Blaze photonics, Endlessly Single Mode PCF: ESM-12-01

[4] CUDOS MOF utility, http://www.physics.usyd.edu.au/cudos/mofsoftware/

[5] Ferrando A., Silvestre E., Miret J.J., Andres P. (2000), Donor and acceptor guided modes in photonic crystal fibers, Optics Letters 25(18), pp. 1328-1330

[6] Foroni M., Cutoff properties of large-mode-area photonic crystal fibers, Information Engineering Department, University of Parma

[7] Koshiba M., Saitoh K. (2004), Applicability of classical fiber theories to holey fibers, Optics Letters, Vol. 29, No. 15, August 1, pp. 1739-1741

[8] Saitoh K., Tsuchida Y., Koshiba M., Mortensen N. A. (2005), Endlessly single-mode holey fibers: the influence of core design, Optics Express, Vol. 13, No. 26, Dezember 26, pp. 10833-10839

[9] Mortensen N. A. (2002), Effective area of photonic crystal fibers, Optics Express, Vol. 10, No. 7, April 8, pp. 341-348

[10] Mortensen N. A., Nielsen M.D., Folkenberg J.R., Peterson A., Simonsen H.R. (2003), Improved large-mode-area endlessly single-mode photonic crystal fibers, Optics Letters, Vol. 28, No. 6, March 15, pp. 393-395

[11] Peyrilloux A., Fevrier S., Marcov J., Berthelop L., Pagnoux B., Sansonetti P. (2002), Comparison between the finite element method, the localized function method and a novel equivalent averaged index method for modelling photonic crystal fibers, Journal of optics A, pure appl. opt. set 4

[12] Uranus H.P., Hoekstra H.J.W.M., van Groesen E. (2004), Modes of an endlessly single-mode photonic crystal fiber: a finite element investigation, Proceedings Symposium IEEE/LEOS Benelux Chapter, Ghent, pp. 311-314

[13] White T.P., McPhedran R.C., de Sterke C.M., Botten L.C., Steel M.J. (2001), Confinement losses in microstructured optical fibers, Optics Letters, Vol. 26, No. 21, November 1, pp. 1660-1662

[14] Zagari J., Argyros A., Issa N.A., Barton G., Henry G., Large M.C.J, van Eijkelenborg M.A. (2004),Small-core single-mode microstructured polymer optical fiber with large external diameter,Optics Letters, Vol. 29, No.8, April 15, pp. 818-826

[15] Zolla F., Renversez G., Nicolet A., Kuhlmey B., Guenneau S., Felbacq D. (2005), Foundations of photonic crystal fibres, Imperial College Press, ISBN 1-86094-507-4